

An Analytical Methodology for the Study of the Transparent Coatings Present on the Surface of Post-Byzantine Icons

Olga Katsibiri, ¹ Demetra Lazidou, ² and Russell F. Howe ³

¹ Department of Chemistry, University of Aberdeen, Meston Walk, Old Aberdeen, Aberdeen AB24 3UE, Scotland, U.K.,

o.katsibiri@abdn.ac.uk, Web site: <http://www.abdn.ac.uk/chemistry>

² Head of Icon Conservation Laboratory, Museum of Byzantine Culture, 2 Stratou Avenue, P.O. Box 50047, 54013 Thessaloniki, Greece, protocol@mbp.culture.gr, Web site: <http://www.mbp.gr>

³ Department of Chemistry, University of Aberdeen, Meston Walk, Old Aberdeen, Aberdeen AB24 3UE, Scotland, U.K., r.howe@abdn.ac.uk, Web site: <http://www.abdn.ac.uk/chemistry>

Abstract - The surface of icons was usually protected by repeatedly applied layers of varnish. Moreover, the colours of the underlying paint layers were sometimes saturated by paint films of glaze. These mostly transparent coatings often cover the original aspect of the icons and complicate their conservation treatment. This study aims at developing an analytical methodology for the characterisation of the surface coatings on a number of Greek post-Byzantine icons by using microscopic, mass spectrometric, and spectroscopic techniques. The results have shown that the aged layers of varnish and glaze contain various mixtures of diterpenoid and triterpenoid resins, linseed oil, a lead-containing dryer, egg, and beeswax. Furthermore, the interaction of the coatings with each other and with the paint layers underneath has also been studied.

Keywords: post-Byzantine, icons, surface coatings, varnishes, glazes, light microscopy, EI-DTMS, imaging-SR-FTIR

Introduction

Byzantine art was predominantly manifested in the representations of religious subjects on wooden panels, the so-called icons. These pictures were closely connected to the life of the Orthodox Church by being an integral part of the liturgy and the circle of festivals. The use of icons was also very popular in domestic devotion, owing to their portability and easy transportation [1,2]. Their production and

An Analytical Methodology for the Study of the Transparent Coatings Present on the Surface of Post-Byzantine Icons

Olga Katsibiri, ¹ Demetra Lazidou, ² and Russell F. Howe

eneration began in the early Byzantine age that extended from 330 to 1453, but also continued after the fall of the Empire in the so-called post-Byzantine era [3,4].

The surface of completed icons was normally protected from the environment (light, humidity, air pollutants, and dust) and from the risk of mechanical damage by thick layers of varnish. In several cases, paint films of glaze were also applied prior to varnishing as part of the actual painting process. In a combined action these transparent coatings saturated the colours of the underlying paint layers by modifying their tones and by creating a surface of even gloss. Ageing, the accumulation of surface dirt, and the heat and soot produced by candles had a substantial effect on their appearance. In an attempt to restore their function, new such coatings were added on top by time-to-time restorers. This resulted today in icons that are smothered with multiple, mostly transparent layers often covering their original aspect [5]. During restoration the effects of this practice become more evident, especially when the treatment involves removal or partial preservation of these coatings (Fig. 1).

The present study aims at giving insights into a number of issues regarding the characterisation of superimposed surface coatings. For this particular project, a number of Greek post-Byzantine icons painted after the 16th century were specifically selected and sampled from the collection of the Museum of Byzantine Culture in Thessaloniki, Greece.

The stratigraphy of the samples was first viewed in cross-sections and the nature of the coatings identified using light microscopy (LM). Their chemical composition was then determined by electron ionisation direct temperature resolved mass spectrometry (EI-DTMS). This technique led to the detection of the organic compounds with some of their degradation products formed during ageing, as well as of certain inorganic materials. Some of the results were also confirmed by on-line tetramethylammonium hydroxide methylation Curie-point pyrolysis gas chromatography mass spectrometry (Py-TMAH-GC/MS).

After establishing the chemical composition, the interaction of these coatings with each other and with the underlying paint layers was examined. Imaging specular reflectance Fourier transform infrared spectroscopy (imaging-SR-FTIR) supplied information on the organic functional group distribution throughout the layers, as well as on certain inorganic species present. In several cases, metal carboxylates formed in glaze and paint layers were identified, and in one case the results were further confirmed by imaging time-of-flight secondary ion mass spectrometry (imaging-TOF-SIMS). Moreover, the metal constituents of a glaze layer were detected by scanning electron microscopy – energy dispersive X-Ray spectroscopy (SEM-EDX).

An Analytical Methodology for the Study of the Transparent Coatings Present on the Surface of Post-Byzantine Icons

Olga Katsibiri, ¹ Demetra Lazidou, ² and Russell F. Howe

The results obtained from the above analysis led to the proposal of an analytical methodology that can be used to characterise the transparent coatings present on the surface of icons.

Experimental

Samples

Five Greek post-Byzantine icons were selected on the basis of the presence on them of superimposed surface coatings and of various surface phenomena. Thirty samples of approximate $100\ \mu\text{m}^2$ each were collected for examination from areas that had not been extensively overpainted or undergone major restoration treatment.

After observing the samples under the stereomicroscope, cross-sections were prepared by mounting them in Technovit® 2000 LC, a one-component methacrylate that polymerises in blue light. Wet grinding with silicone carbide (SiC) sheets followed and their surface was dry-polished on Micro-Mesh® cloths [6].

LM

The cross-sections were observed under a Leica DMRX analytical microscope (Leica Inc., Wetzlar, Germany) with a resolution of approximately $1\ \mu\text{m}$. The microscope was equipped with a 100 W halogen projection lamp for visible (VIS) incident light microscopy in bright and dark field illumination. For ultra-violet (UV) fluorescence microscopy, an Osram HBO 50 high-pressure mercury lamp and a Leica filter D (excitation 360-425 nm, emission $> 460\ \text{nm}$) were used. The cross-sections were recorded in images with a Nikon DXM1200 digital still camera (Nikon Instech Co., Ltd., Japan).

EI-DTMS

Sub-sampled layers of about $10\text{-}50\ \mu\text{g}$ were made into a suspension in a mini-mortar using aliquots of ethanol. Approximately $2\text{-}5\ \mu\text{l}$ of the suspension was transferred to the platinum/rhodium (90:10) filament ($\varnothing\ 100\ \mu\text{m}$) of the probe, dried *in vacuo*, and inserted directly into the ion source of a JEOL JMS-SX/SX102A tandem mass spectrometer. The filament was resistively heated by ramping the current at a rate of $0.5\ \text{A/min}$, and the temperature linearly increased from ambient to approximately $800\ ^\circ\text{C}$ in 2 min. Ions were generated using $16\ \text{eV}$

electron ionisation. The mass spectrometer was scanned over a m/z range of 20-1000 using a 1 s cycle time and the data were processed using a JEOL MP-7000 data system [7].

Py-TMAH-GC/MS

Sub-sampled layers of about 10-50 μg were placed in a gas chromatographic vial together with 10 μl of 2.5% aqueous solution of TMAH. The vial was capped and sonicated for 5 min. Approximately 2-5 μl of the sample suspension was applied to the rotating 610 °C Curie-point wire and the sample dried *in vacuo*. The ferromagnetic wire was inductively heated for 9 s in a 1 MHz RF field to its Curie-point temperature. Pyrolysis fragments were flushed into the pre-column/column set-up mounted in a Fisons gas chromatograph (series HRGC MEGA 2) and coupled directly to the ion source of a JEOL JMS-SX/SX102A tandem mass spectrometer via an in-house built interface kept at 290 °C. A venting module was also installed between the pre-column and the analytical column to eliminate most of the unreacted TMAH. This module was open for 10 sec during pyrolysis to remove the reagent while concentrating the sample on the retaining pre-column. Helium was used as carrier gas at a flow rate of 2 ml/min. A JEOL MS-MP9020D data system was used for data acquisition and the electron ionisation was carried out at 70 eV.

Pre-column: Chrompack VF-1ms, length 3 m, i.d. 0.32 mm, film thickness 0.10 μm . Analytical column: Chrompack VF-5ms, length 30 m, i.d. 0.32 mm, film thickness 0.50 μm .

Oven programme: 50 °C (2 min) – 6 °C/min – 320 °C (10 min).

Imaging-SR-FTIR

The cross-sections were analysed in specular reflectance mode on a Bio-Rad Stingray system (Bio-Rad, Cambridge, MA, USA). This combines a Bio-Rad FTS 6000 spectrometer equipped with a Bio-Rad UMA 500 infrared microscope and a 64 x 64 element mercury cadmium telluride (MCT) focal plan array detector (Santa Barbara Focal Plane, Goleta, CA, USA). Images of a 400 x 400 μm area were recorded with a spatial resolution of 6-7 μm , spectral resolution of 16 cm^{-1} (approximately 500 interferosteps), under sampling ratio (UDR) of 4, step-scan frequency of 1 Hz, and a step distance of the interferometer at UDR 4 of 1.266 μm . The interferometer was controlled, the images acquired, and the resulting dataset processed using Bio-Rad Win-IR Pro 2.5 and ImageIR 2.1 software. A zinc selenide (ZnSe) window was chosen for calibration and background acquisition because of its nearly constant reflectance in the mid-IR

range. The specular reflectance spectra were transformed to absorbance spectra using the Kramers-Kronig transformation [8].

Imaging-TOF-SIMS

A single cross-section was analysed on a Physical Electronics (Eden Prairie, MN, USA) TRIFT II time-of-flight secondary ion mass spectrometer. The cross-section was first rinsed in hexane to reduce contamination of silicones. To prevent large variations in the extraction field over the large insulation surface area, a non-magnetic stainless plate with slits (1 mm) was placed on top of the cross-section. The surface was scanned with a 15 keV primary ion beam from an $^{115}\text{In}^+$ liquid metal ion gun. The pulsed beam was non-bunched, with a pulse width of 20 ns, a current of 60 pA, and a spot size of approximately 120 nm. The static SIMS measurements were taken in both positive and negative mode [9].

SEM-EDX

The cross-sections were carbon coated on a CC7650 Polaron Range coater with carbon fibre (Quorum Technologies, East Sussex, UK) to improve surface conduction. Measurements were performed on a XL30 SFEG high-vacuum electron microscope equipped with a field emission source (FEI, Eindhoven, The Netherlands) and an EDX system from EDAX (Tilburg, The Netherlands). Information on elemental composition was obtained by spot analysis. Backscatter electron (BSE) images were taken at 20 kV acceleration voltage, 5 mm eucentric working distance, and a spot size of 3, corresponding to a beam diameter of 2.2 nm with current density of approximately 130 pA. EDX analysis was performed at a spot size of 4 (beam diameter 2.5nm, current density 550 pA) and at acceleration voltage of 22 kV to obtain higher count rate.

Results and Discussion

LM

All cross-sections consist of surface coatings of variable colour and thickness. In the majority of cases, these have been applied to the icons at different stages with an unknown time difference between them. Their strong fluorescence in UV-light illumination indicates the presence of aged drying oils and/or natural resins [10]. In one case, however, a dark-coloured layer shows no fluorescence and was therefore assumed to be a glaze (Fig. 2a,b) [11]. The presence of

intermediate surface-dirt layers makes the borderlines of the coatings visible, as does in some cases the variation in intensity of fluorescence (Fig. 2c,d). In other cases, the coatings have contracted into a wavy shape or have lost their layer sequence and turned into a mixture of material. This indicates that they have been dissolved by means of a solvent, and/or by new coatings added on top of them, in which case they would be affected by the thinning agent. Another possibility is that they have been scorched from candles lit close to them.

Regarding the underlying paint layers, an interesting observation was made on one cross-section. The surface of a white-paint layer is covered by small crater-like voids and protrusions of whitish material (Fig 3). This phenomenon is caused by the formation and expansion out of the surface of a painting of metal soaps, as reported in several cases in the literature [12-14].

EI-DTMS and Py-TMAH-GC/MS

The attempts to manually separate the surface coatings under the stereomicroscope were unsuccessful due to the strong adhesion between them. Therefore, depending on their occurrence in sampling, one or more of them were analysed in each run.

The mass spectra and chromatograms supplied compositional information on the molecular scale on the compounds present in the surface coatings (Fig. 4). Highly oxidised diterpenoid acids with the abietane skeleton, larixol or larixyl acetate, communic acid with its only low-molecular-mass degradation product, and oxidised triterpenoids were detected. Furthermore, free and/or network-bonded fatty acids (FAs), FA-oxidation products, and the isotopes of lead were identified. Finally, features characteristic of protein-derived compounds, cholesterol with some of its oxidation and degradation products, and the monoesters formed by the C16:0 FA with the series of alcohols were detected. The compounds and the m/z values of the most significant molecular and fragment ions seen in the EI-DTMS spectra are listed in the Table, and some molecular structures are shown in Fig. 5 [15-23].

The compounds in the above Table indicate that the surface coatings contain oxidised diterpenoid resins from the *Pinaceae* family in some cases specifically identified as Venice turpentine, aged sandarac or Manila copal, oxidised triterpenoid resins, an aged drying oil, lead, aged egg, and beeswax. Based on the ratio of the C16:0 to the C18:0 FA peaks (P/S), the drying oil in all cases seems to be linseed oil [24]. Finally, in the white-coloured paint layer

where the voids and protrusions were observed (Fig. 3), linseed oil was detected together with the pigment of lead white.

Imaging-SR-FTIR and Imaging-TOF-SIMS

IR spectra were collected from the different surface coatings in the cross-sections, and the intensity of specific absorption bands was imaged in false colour plots (Figs. 6,7). These are maps that show the distribution of a particular absorption band over the surface of a cross-section using false colours. More specifically, the blue colour represents a low intensity of the indicated absorption band, while the red area corresponds to a high intensity [8].

A number of absorption bands characteristic of oxidised resins and polymerised drying oils were identified and localised, thus confirming the results from the mass spectrometric and chromatographic analysis. Moreover, the presence of proteinaceous material, as well as of some particles containing carbonates, sulphates, and silicates from surface impurities was also detected (Figs. 6,7).

In the cross-section where the glaze layer was observed (Fig. 2a,b), copper carboxylates were detected. These are formed by copper(II) ions extracted from copper pigments by fatty and terpenic acids present in oleoresinous media, and indicate that this is a copper-based glaze [14,25]. On the other hand, in the lead-white layer where the voids and protrusions were observed (Fig. 3), metal carboxylates were detected. These are formed upon reaction of the carboxylic acids present in oil with the metal ions of lead contained in the paint layer.

SEM-EDX

Single point EDX of the cross-section where the glaze layer was observed (Fig. 2a,b) confirmed the presence of copper. Hence, a copper pigment has been used for its preparation, presumably verdigris [11].

Conclusions

Based on the above analytical results, it can be concluded that the icons examined are covered with aged layers of varnish and glaze. The diterpenoid resins detected may be Venice turpentine or colophony, as well as sandarac or Manila copal, the latter however being fairly unlikely to have been used in icons. The triterpenoid resins on the other hand can be dammar or mastic, the former being only introduced into the market in 1829 [17]. The linseed oil may be part of an oil varnish or may have been applied as a separate coating. Furthermore, lead seems to have been added to it as a dryer. The egg detected is likely to have been used for conservation purposes or in some cases it

may be due to contamination. Its use, however, in the preparation of varnishes and glazes cannot be ruled out. Finally, the beeswax seems to be part of a varnish, for instance as additive to dammar to reduce its highly glossy effect. In an extreme case, it can be residue from candles used in churches or domestic veneration.

In the case of the glaze layer (Fig. 2a,b), the presence of Venice turpentine and verdigris suggests that this is a copper resinate. Plain linseed oil seems to have been used as surface coating over the lead-white layer where the formation of lead soap aggregates has caused crater-like voids and protrusions to appear (Fig. 3). This is supported by the fact that the phenomenon appears to be more intense on the surface rather than at the bottom of the paint layer.

The detailed information obtained through combined analysis provided a clear image of the state, chemical composition, and the interaction of the aged surface coatings on the icons examined. The combination of the above techniques can therefore form a methodology to be used as guideline for the characterisation of the transparent coatings present on the surface of icons. An attempt to further supplement this study was made by using micro-Raman spectroscopy, but the strong fluorescence of the materials analysed prevent it from adding any meaningful information.

Acknowledgements

The majority of analysis described in the present study was carried out at the laboratories of the FOM Institute for Atomic and Molecular Physics, Amsterdam, The Netherlands. The Greek State Scholarships Foundation provided Olga Katsibiri with a full scholarship. Further support was obtained from the COST Action G8 and the Scottish International Educational Trust. We would also like to thank the ORMYLIA Art Diagnosis Centre, Chalkidiki, Greece for assistance with sampling and with the analytical results.

References

- [1] Baggle, J., 1995. *Doors of Perception - Icons and Their Spiritual Significance*. N. York: St. Vladimir's Seminar Press, pp. 1-32, 87-98.
- [2] Cormack, R., 2000. *Byzantine Art*. Oxford: Oxford University Press, pp. 2-6, 210-217.
- [3] Haldon, J., 2002. *Byzantium: A History*. Gloucestershire: Tempus Publishing, pp. 9-12.

- [4] Iorga, N., 2000. *Byzantium after Byzantium*. Oxford: The Center for Romanian Studies.
- [5] Sendler, E., 1999. *The Icon: Image of the Invisible - Elements of Theology, Aesthetics and Technique*. Hong Kong: Oakwood Publications, pp. 216-217.
- [6] Khandekar, N., 2003. Preparation of Cross-Sections from Easel Paintings. *Reviews in Conservation*, **4**, 52-63.
- [7] Boon, J.J., 1992. Analytical Pyrolysis Mass Spectrometry: New Vistas Opened by Temperature-Resolved In-Source PYMS. *International Journal of Mass Spectrometry and Ion Processes*, **118/119**, 755-787.
- [8] Van der Weerd, J., Brammer, H., Boon, J.J., and Heeren, R.M.A., 2002. Fourier Transform Infrared Microscopic Imaging of an Embedded Paint Cross-Section. *Applied Spectroscopy*, **56**, 275-283.
- [9] Keune, K., and Boon, J.J., 2004. Imaging Secondary Ion Mass Spectrometry of a Paint Cross Section Taken from an Early Netherlandish Painting by Rogier van der Weyden. *Analytical Chemistry*, **76**, 1374-1385.
- [10] De la Rie, E.R., 1982. Fluorescence of Paint and Varnish Layers (Part II). *Studies in Conservation*, **27**, 62-69.
- [11] Van den Berg, K.J., Van Eikema Hommes, M.H., Groen, K.M., Boon, J.J., and Berrie, B.H., 2000. On Copper Green Glazes in Paintings. In *Art et Chimie, la Couleur, Actes du Congrès*. Paris: CNRS Éditions, pp.18-21.
- [12] Van der Weerd, J., Boon, J.J., Geldof, M., Heeren, R.M.A., and Noble, P., 2002. Chemical Changes in Old Master Paintings: Dissolution, Metal Soap Formation and Remineralisation Processes in Lead Pigmented Paint Layers of 17th Century Paintings. *Zeitschrift für Kunsttechnologie und Konservierung*, **16**, 35-51.
- [13] Plater, M.J., De Silva, B., Gelbrich, T., Hursthouse, M.B., Higgitt, C.L., and Saunders, D.R., 2003. The Characterisation of Lead Fatty Acid Soaps in "Protrusions" in Aged Traditional Oil Paint. *Polyhedron*, **22**, 3171-3179.
- [14] Robinet, L., Corbeil, M.C., 2003. The Characterisation of Metal Soaps. *Studies in Conservation*, **48**, 23-40.
- [15] Van den Berg, K.J., Boon, J.J., Pastorova, I., and Spetter, L.F.M., 2000. Mass Spectrometric Methodology for the Analysis of Highly Oxidized Diterpenoid Acids in Old Master Paintings. *Journal of Mass Spectrometry*, **35**, 512-533.
- [16] Scalarone, D., Van der Horst, J., Boon, J.J., and Chiantore, O., 2003. Direct-Temperature Mass Spectrometric Detection of Volatile Terpenoids and Natural Terpenoid Polymers in Fresh and Artificially Aged Resins. *Journal of Mass Spectrometry*, **38**, 607-617.
- [17] Van der Doelen, G.A., Van den Berg, K.J., and Boon, J.J., 1998. Comparative Chromatographic and Mass-Spectrometric Studies of

Triterpenoid Varnishes: Fresh Material and Aged Samples from Paintings. *Studies in Conservation*, **43**, 249-264.

[18] Van der Doelen, G.A., and Boon, J.J., 1995. Mass Spectrometry of Resinous Compounds from Paintings: Characterisation of Dammar and Naturally Aged Dammar Varnish by DTMS and HPLC/MS. In *Resins: Ancient and Modern, Preprints of the SSCR's 2nd Resins Conference, Aberdeen 13-14 September 1995*. Aberdeen: Scottish Society for Conservation & Restoration, pp. 70-75, Errata.

[19] Van den Berg, J.D.J., 2002. *Analytical Chemical Studies on Traditional Linseed Oil Paints*. Ph.D. University of Amsterdam: FOM-Institute AMOLF, pp. 89-130; (<http://www.amolf.nl/publications/theses/>).

[20] Van Arendonk, J.J.M.C., Niemann, G.J., and Boon, J.J., 1997. The Effect of Enzymatic Removal of Proteins from Plant Leaf Material as Studied by Pyrolysis-Mass Spectrometry: Detection of Additional Protein Marker Fragment Ions. *Journal for Analytical and Applied Pyrolysis*, **42**, 33-51.

[21] Van den Brink, O.F., 2001. *Molecular Changes in Egg Tempera Paint Dosimeters as Tools to Monitor the Museum Environment*. Ph.D. University of Amsterdam: FOM-Institute AMOLF, pp. 29-54, 107-121; (<http://www.amolf.nl/publications/theses/>).

[22] Boon, J. J., Peulvé, S. L., Van den Brink, O. F., Duursma, M. C., and Rainford, D., 1997. Molecular Aspects of Mobile and Stationary Phases in Ageing Tempera and Oil Paint Films. In *Early Italian Paintings: Techniques and Analysis, Symposium, Maastricht, 9-10 October 1996*. Maastricht: Limburg Conservation Institute, pp. 35-56.

[23] Bonaduce, I., and Colombini, M.P., 2004. Characterisation of Beeswax in Works of Art by Gas Chromatography-Mass Spectrometry and Pyrolysis-Gas Chromatography-Mass Spectrometry Procedures. *Journal of Chromatography A*, **1028**, 297-306.

[24] Mills, J.S., and White, R., 1999. *The Organic Chemistry of Museum Objects*. Oxford: Butterworth-Heinemann, pp. 171-172.

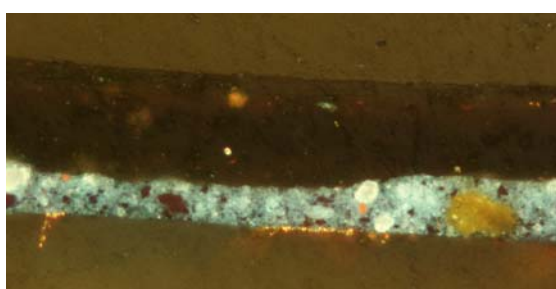
[25] Gunn, M., Chottard, G., Rivière, E., Girerd, J.J., and Chottard, J.C., 2002. Chemical Reactions Between Copper Pigments and Oleoresinous Media. *Studies in Conservation*, **47**, 12-23.

Table – List of the most characteristic m/z values in the EI-DTMS spectra of the surface coatings (molecular ions in italics, most prominent ions underlined)

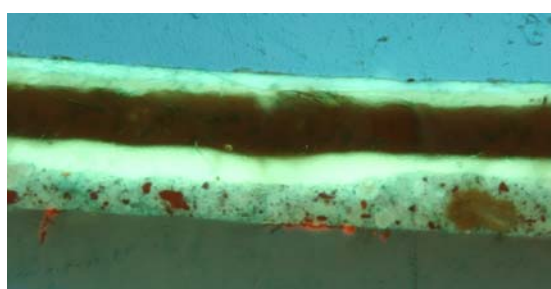
Compound	Characteristic EI ion peaks (<i>m/z</i>)
Dehydroabietic acid (DHA)	239, <u>285</u> , 300
15-hydroxy-DHA	237, 255, <u>301</u> , 316
7-oxo-DHA	<u>253</u> , 299, <u>314</u>
7,15-dihydroxy-DHA	<u>235</u> , 332
15-hydroxy-7-oxo-DHA	251, 312, <u>315</u> , 330
Larixol/larixyl acetate	<u>255</u> , <u>270</u> , 273, 288
Communic acid	<u>175</u> , <u>221</u> , 287, 302
19-norlabda-8(20),13-dien-15-oic acid	<u>275</u> , <u>290</u>
Dammaradienone	<u>109</u> , 205, 424
Dammaradienol	<u>109</u> , 426
Hydrodammarone	<u>109</u> , 315, 355, 424
Dammarenolic acid	<u>109</u> , 440
Hydroisopropylmethyltetrahydrofuran side-chain of oxidised dammarane-skeleton molecules (ocotillone-type molecules)	<u>143</u> , <u>399</u> , 440
Oxidised dammarane-skeleton molecules with the lactonised side-chain	99, <u>414</u>
Moronic/oleanonic/ursonic acids	189, 203, 235 (moronic acid), 248, 409, 454
28-nor-olean-18-en-3-one	<u>163</u> , 191, 410
C16:0 fatty acid (FA)	256
C18:0 FA	284
Alkylated benzenes	91 (toluene), 105 (xylene)
FA components from fragmentation at C7	129
C9 diacid	98, 152 (diacylium ion)
Isotopes of Pb	206, 207, <u>208</u>
Indole	<u>117</u>
Methylindole	<u>131</u>
Ethylindole	<u>145</u>
Phenol	<u>94</u>
Methylphenol	<u>108</u>
4-(4-hydroxyphenyl)-phenol	<u>186</u>
Cholesterol	386
Cholestadiene	368
Cholestadienone	382
Cholestenone	384
Hydroxycholestenone	400
Monoesters of the C16 FA with the C24- C34 alcohols	592 (C40), 620 (C42), 648 (C44), 676 (C46), 704 (C48), 732 (C50)



Fig. 1 – The icon of St. Minas, 18th century - Thick layers of varnish as seen after partial cleaning



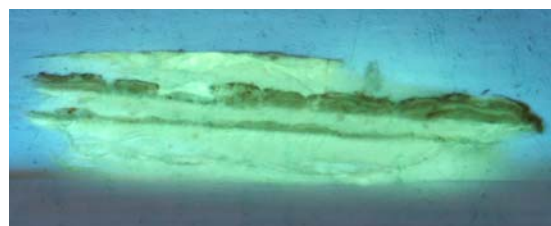
(a)



(b)



(c)



(d)

Fig. 2 – Light microscopic images of two cross-sections containing surface coatings; upper row: magnification 320x, illumination in (a) VIS incident light, (b) UV light; lower row: magnification 125x, illumination in (c) VIS incident light, (d) UV light



Fig. 3 – The icon of St. George, 17th century - Protrusions and crater-like voids due to the formation of lead soaps in the surface of a lead-white layer

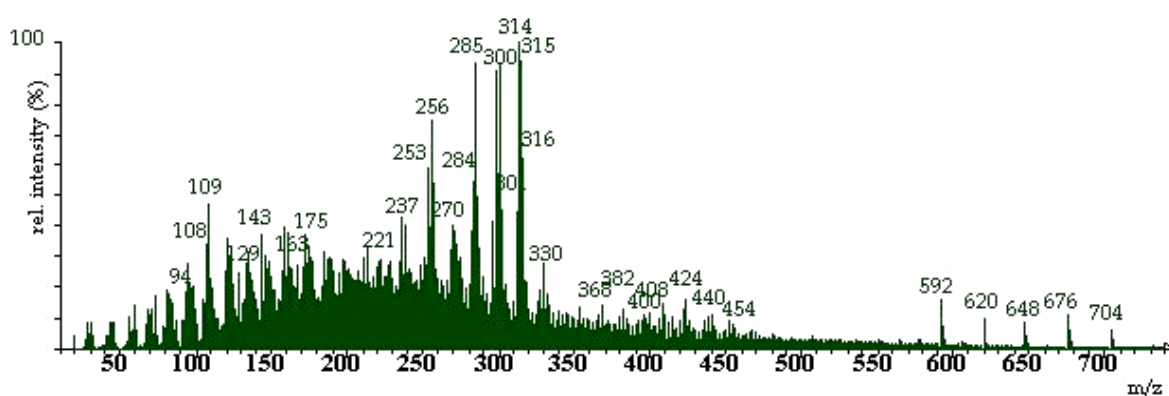


Fig. 4 – EI-DTMS summation spectrum of the sample in Figure 2c,d

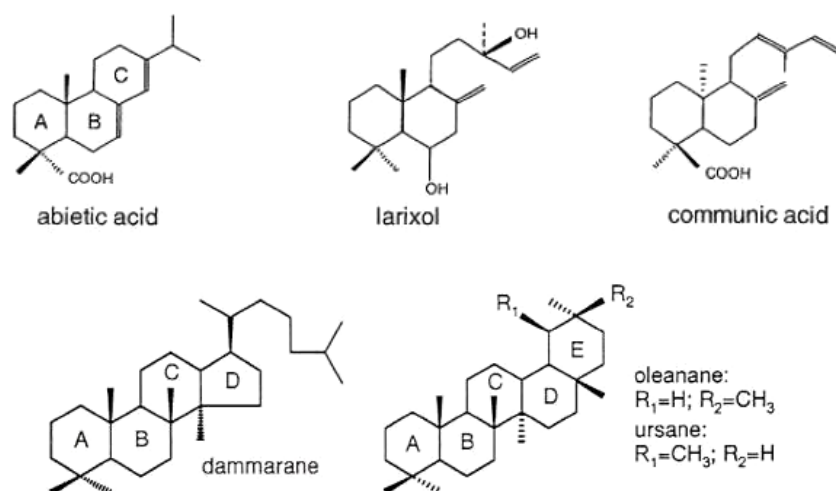


Fig. 5 – Molecular structures of some compounds identified in the EI-DTMS spectra of the surface coatings

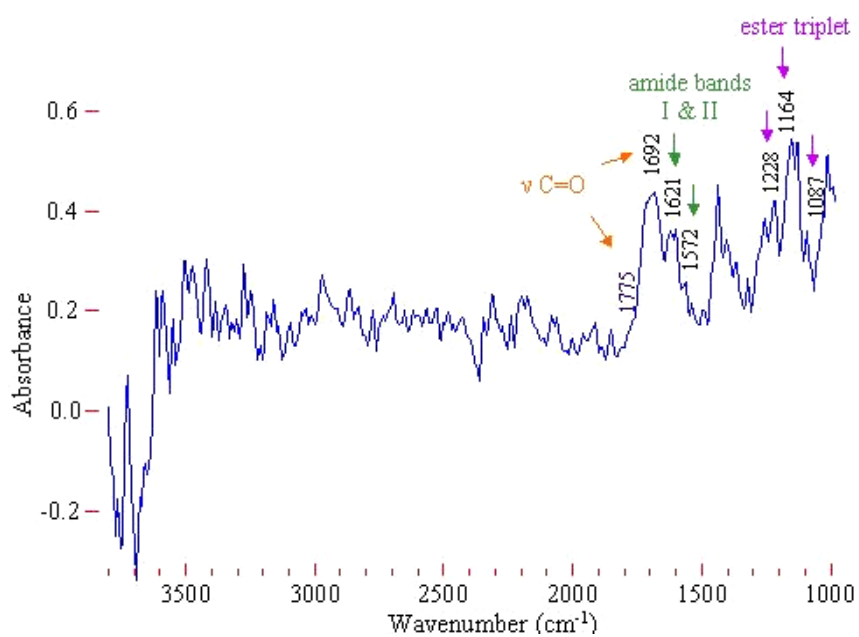
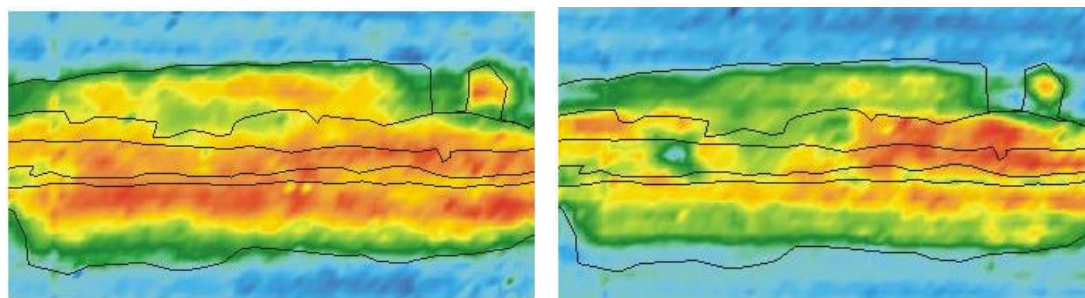


Fig. 6 – SR-FTIR spectrum of a surface coating in the cross-section of Figure 2c,d



(a) 1692 cm⁻¹

(b) 1621 cm⁻¹

Fig. 7 – False colour plots of the cross-section in Figure 2c,d with a map of the different surface coatings, imaging the intensity of absorption at (a) 1692 cm⁻¹ for the ν C=O of natural resins (b) 1621 cm⁻¹ for the amide band I of proteins